FUDMA Journal of Sciences (FJS)
ISSN online: 2616-1370
ISSN print: 2645 - 2944
Vol. 9 No. 11, November, 2025, pp 196 – 208
DOI: https://doi.org/10.33003/fjs-2025-0911-3740

THE IMPACT OF MULTIFACETED VACCINATION INTERVENTIONS ON MEASLES ERADICATION: A BEHAVIORAL ANALYSIS OF THE SEITRV EPIDEMIC MODEL

***[1]Mutairu Kayode Kolawole and [2]Bukola Olayemi Akin-Awoniran**

[1]Osun State University, Osogbo
[2]Osun State College of Technology Esa-Oke

*Corresponding Author's Email: mutairukolawole@uniosun.edu.ng

ABSTRACT

Despite the effectiveness of the vaccine, measles is still a major worldwide health concern. Human behavior, including vaccine reluctance and reactions to health initiatives, is examined in this study. This study uses a thorough SEITRV (Susceptible–Exposed–Infectious–Treated–Recovered–Vaccinated) model to examine how different vaccination campaigns impact measles transmission via the lens of human behavior. Using both epidemiological and behavioral characteristics, an SEITRV model was created to mimic the spread of measles. We modeled treatments including treatment availability, education campaigns, and mass and targeted immunization. Simulations assessed how public behavior affects the spread of disease using data from previous outbreaks. According to simulation studies, vaccination intervention has a major impact on how measles outbreaks develop. Models that took vaccination awareness into account. Strategies that combined strong public education with high vaccination rates, in particular, showed the biggest drops in disease prevalence. These results highlight how ineffective vaccination coverage is on its own in controlling disease This study emphasizes that mass vaccination for controlling measles and behavioral variables like vaccination reluctance and public response to health campaigns must also be addressed by public health methods. The efficacy of disease control initiatives is increased when medical interventions are combined with focused initiatives to change public perceptions and behavior. Therefore, effective measles containment and eventual eradication require a dual focus on clinical and behavioral interventions.

Keywords: Measles, Vaccine, SEITRV model, Vaccination, Educational programme, Eradication

INTRODUCTION

The fast-spreading Morbillivirus is what causes measles and this disease is well known for causing serious health problems. Generally, running a fever, getting a rash, red eyes or cough appear about 8–12 days following contact. Since recent outbreaks happened in areas where the vaccine is less common, it is clear we must learn more about Disease A and see how spreading awareness affects its spread. Since the disease spreads very fast, several strategies are necessary to ensure it is completely wiped out (WHO, 2025; Yunus& Olayiwola, 2025; Adewole (2022); Kumar et al., 2022; Peter et al., 2024). Epidemiologic tools with real information are practical for studying how measles spreads, but carefully looking at people's actions explains how epidemics, population size and control strategies fit together. Control strategies can make it clearer how disease spreads and is controlled in a population by lowering the disease burden while staying within resource constraints and being aware of the main characteristics of the epidemiological models (Wireko et al., 2024; Phillipp 2020; Adewale et al., 2014). Many studies have shown that mathematical models are very helpful in explaining and managing the spread of infectious diseases (Kolawole, 2024; Kolawole & Olayiwola, 2016; Kolawole et al., 2022a; Kolawole et al., 2022b; Olayiwola et al., 2025). They create order in understanding transmission, project different results using different examples and show the impact of different strategies. By changing epidemiological data into measurable factors such models assist in deciding effective public health policies and applicable actions (Vynnycky et al., 2018; Oh et al., 2022; Suwoyo et al., 2023; Kolawole et al., 2023; Yunus & Olayiwola, 2025). As a result of these insights, response and readiness are improved and limited resources are better distributed to benefit most people. Vaccination plays a key role in preventing different types of infectious diseases from spreading. To be effective, vaccination programs depend on reaching and serving individuals equally and they must have high population coverage (Kolawole, 2025; Yunus & Olayiwola, 2025a; Yunus & Olayiwola, 2025b; Yunus & Olayiwola, 2024; Olayiwola et al., 2023; Plans-Rubio, 2020). Mathematical studies have shown that using vaccines can bring about a drop in the spread of diseases, fewer cases of sickness and a possible end to diseases such as measles. They also underline the fact that both public participation and a well-run process matter and that public health depends on a balance between medical factors and the parts of life that affect health. Examining how vaccination supports disease control and elimination stresses immunization's major role in building the overall health of people everywhere. These epidemics are frequently caused by issues including vaccine hesitancy, unequal vaccination coverage, and vaccine administration delays. It is crucial to comprehend how human behavior shapes vaccine dynamics in order to eradicate measles. An innovative SEITRV (Susceptible–Exposed–Infectious–Treated–Recovered–Vaccinated) epidemic model that integrates behavioral responses into measles transmission and control is presented in this work. This paradigm incorporates several vaccination techniques, such as reactive campaigns and routine immunization, treatment-seeking behavior, and public awareness, which is not the case with traditional models. The model mimics the ways in which these complex actions interact with community behavior to affect how measles epidemics develop. The novelty of this research lies in its comprehensive behavioral integration within a compartmental epidemic model and its ability to assess the effectiveness of combined interventions. This approach provides deeper insights into the design of more adaptive and targeted vaccination policies, helping public health authorities

maximize the impact of immunizations programme and move closer to global measles eradication.

MATERIALS AND METHODS

Model Formulation

Based on the Adewole (2022), this paper then develops a compartmental mathematical model to explain the dynamics of transmission of measles in a population. It includes effectively the major disease phases and primary public health measures, including treatment and vaccination, by subdividing the population into six compartments, Susceptible (S), Exposed (E), Infectious (I), Treated (T), Recovered (R), and Vaccinated (V). It describes infection by contact, the process of exposure to infectiousness, treatment, recovery, vaccination and loss of immunity. The important control measures, which include vaccination, treatment, and creation of awareness among the population, are clearly included. Another assumption that the model takes into account is relapse because of immunity diminution and natural death. Its dynamics are biologically realistic as well as mathematical consistent, well-posed both analytically and numerically, and offer a solid mathematical platform to comprehend the dynamics of measles and test interventional strategies. The system of equations is thus depicted in (1) below with model description below in table 1 which give description of parameters, values, and references

$$\begin{aligned}
\frac{dS}{dt} &= \mu N - \beta\frac{I}{N}S - (\alpha+\rho+\varphi)S \\
\frac{dE}{dt} &= \beta\frac{I}{N}S - (\sigma+\varphi)E \\
\frac{dI}{dt} &= \sigma E - (\gamma_1+\delta+\varphi)I \\
\frac{dT}{dt} &= \rho S + \delta I - (\gamma_2+\varphi)T \\
\frac{dR}{dt} &= (\theta+\gamma_1)I + \gamma_2 T - (\varphi+\omega)R \\
\frac{dV}{dt} &= \alpha S - (\varphi+\eta)V
\end{aligned} \quad (1)$$

as $S(t) \geq 0, E(t) \geq 0, I(t) \geq 0, T(t) \geq 0, R(t) \geq 0, V(t) \geq 0$ and is subjected to an initial condition $0 < T \leq 1$

Table 1: Description of Variables

Variable	Description
$S(t)$	Susceptible class
E(t)	Exposed class
I(t)	Infected class
T(t)	Treated class
R(t)	Recovered class
V(t)	Vaccinated class

Table 2: Description of Parameters and Values

Parameter	Description	Values
N	Total population	0.1625
β	Rate of transmission from infected individuals to susceptible individuals	0.001
σ	Rate at which exposed individuals become infectious	0.5
γ_1, γ_2	Recovery rate of infectious individuals	0.2
φ	Natural mortality rate	0.03
δ	Rate of treatment effectiveness i.e. treatment reduces transmissibility or severity	1.0
α	Rate of vaccination	0.0016
ρ	Awareness and enlightenment rate i.e. influences the probability of vaccination and decreases the susceptible population by encouraging self-protection or behavior changes)	0.113
θ	Academic program intervention which promotes better health-seeking behaviour and treatment compliance	1.0126
η	Vaccine waning rate	0.3
ω	Loss of immunity rate	0.5

Existence and Uniqueness of the Model Solution

The model in equation (1), which represents the spread of an epidemic disease within a human population, requires that its parameters be nonnegative for its existence and uniqueness of the model solution. To ensure that the system of differential equations in equation (1) is both mathematically valid and epidemiologically sound, it is important to establish that the model's state variables remain nonnegative. Equation (1) is considered well-defined at the initial point if the initial conditions are nonnegative. $S(0) = s_0, E(0) = e_0, I(0) = i_0, T(0) = t_0, R(0) = r_0, V(0) = v_0$; In that case, the solutions of system (1) will persist in being nonnegative throughout their evolution, $t > 0$ and that these positive solutions are bounded. We thus apply the following theorems.

Theorem 1

Let (x, y) be distinct points of normed linear space $(X, \|\cdot\cdot\cdot\|)$ over $\Re$. Then the map of $p: [0,1] \subseteq \Re \to (X, \|\cdots\|)$ such that $p(\lambda) = \lambda x + (1-\lambda)y$ is continuous on [0, 1].

Proof:

Let $\lambda_0 \in [0,1]$ then $p(\lambda_0) = \lambda_0 x + (1-\lambda_0)y$ for any $\lambda_0 \in [0,1]$, $\|p(\lambda) - p(\lambda_0)\| = \|(\lambda-\lambda_0)x + (\lambda-\lambda_0)y\| \leq |\lambda-\lambda_0|(\|x\| + \|y\|)$ (2)

If $\varepsilon > 0$ is given, let $\delta = \frac{\varepsilon}{\|x\|+\|y\|}$. If $|\lambda-\lambda_0| < \delta$, then the $\|p(\lambda) - p(\lambda_0)\| < \varepsilon$. Therefore, p is continuous at λ_0. Since λ_0 is an arbitrary point in [0, 1]. Then p is continuous on [0, 1]. Let X be a linear space over $\Re$. If (x, y) are distinct points of X, the set $\lambda x + (1-\lambda)y$ lies in $0 \leq \lambda \leq 1$

Hence, the solutions of system (1) are bounded if we consider the total population. The variation in the total population concerning time is given by:

$$N(t) = S(t) + \mathrm{E}(t) + \mathrm{I}(t) + T(t) + \mathrm{R}(t) + V(t) \quad (3)$$

The variation in the total population concerning time is given by:

$$\frac{dN(t)}{dt} = \frac{d}{dt}(S(t) + \mathrm{E}(t) + \mathrm{I}(t) + T(t) + \mathrm{R}(t) + V(t)) \quad (4)$$

Such that

$\frac{dN(t)}{dt} = \mu - \varphi(S + E + I + T + R + V) \Rightarrow N^*(t) \leq \mu - \varphi N$ (5)

Hence, it is obtained that
$N^*(t) + \varphi N \leq \mu$, using the integrating factor concept on the total population N(t) and this leads to
Firstly,
$N(0) = \frac{\mu}{\varphi} + Ke^{-\mu(0)}, K = N(0) - \frac{\mu}{\varphi}$ resulting to
Thus, substituting (6) into (5) as time progressively increases yields:

$\lim_{t\to\infty} N(t) \leq \lim_{t\to\infty}\left[\frac{\mu}{\varphi} + \left(N(0) - \frac{\mu}{\varphi}\right)e^{-\mu t}\right] = \frac{\mu}{\varphi}$ (6)

Then$N(0) \leq \frac{\mu}{\varphi}$, then$N(t) \leq \frac{\mu}{\varphi}$. This is a positive invariant set under the flow described by (6) so that no solution path leaves through any boundary$\Re_+^6$. Hence, it is sufficient to consider the dynamics of the model in the domain$\Re_+^6$. In this region, the model can be considered has be mathematically and epidemiologically well-posed. This shows that the total population and the subpopulation $S(t), E(t), I(t), T(t)R(t), V(t)$of the model are bounded and is a unique solution. Hence, its applicability to studying physical systems is feasible.

Positivity and Boundedness of Model Solution in $\Re_+^6$

This shows that the total population$N(t)$, and the subpopulation $S(t), E(t), I(t), T(t), R(t), V(t)$of the model are bounded and is a unique solution. Hence, its applicability to study physical systems is feasible.

Theorem 2

Suppose $X = x_0$is a space of consecutive real number and which are defined as

$L(x,y) = \left(\sum_{i=1}^{n}|x_i|^{\Omega}\right)^{\frac{1}{\Omega}} \quad \Omega \geq 1$ (7)

X with the metric is called ξ_n^{Ω}space. If $\sum^{\infty}|x|^{\Omega} < \infty$or absolutely convergent and$L(x,y) = \left(\sum_{i=1}^{\infty}|x_i - y_i|^{\Omega}\right)^{\frac{1}{\Omega}}$, then X with this metric is called an ξ^{Ω}space.

Proof:

It can be checked that for each n:

$0 \leq x_1^2 + x_2^2 + x_3^2 + \ldots + x_n^2 \leq (|x_1| + |x_2| + |x_3| + \ldots + |x_n|)^2$ (8)

This will result to;

$x_1^2 + x_2^2 \leq (|x_1| + |x_2|)^2$ (9)

Therefore,

$0 \leq (x_1^2 + x_2^2 + x_3^2 + \ldots + x_n^2)^{\frac{1}{2}} \leq |x_1| + |x_2| + |x_3| + \ldots + |x_n|$,

If $\sum_{n=1}^{\infty}|x_n|$ converges, that is $\sum_{n=1}^{\infty}|x_n|$is absolutely convergent, then

$0 \leq (x_1^2 + x_2^2 + x_3^2 + \ldots + x_n^2)^{\frac{1}{2}} \leq |x_1| + |x_2| + |x_3| + \ldots + |x_n| = \sum_{n=1}^{\infty}|x_n| < \infty$ (10)

Therefore,

$0 \leq x_n = x_1^2 + x_2^2 + x_3^2 + \ldots + x_n^2 \leq [\sum_{n=1}^{\infty}|x_n|] < \infty$ (11)

These sequences $x_n$is monotone increasing and bounded above, it therefore converges. Thus $\sum_{n=1}^{\infty}x_n$converges absolutely, if$x_n \in \xi^1$, then $x_n \in \xi^2$where$\xi^1 \leq \xi^2$. In case of ξ^1 denote the set of all sequences of $x_n$of real numbers such that $\sum_{n=1}^{\infty}x_n$is convergent absolutely. i.e $\sum_{n=1}^{\infty}|x_n| < \infty$whereas ξ^2denote the set of all sequence $x_n$of real numbers such that $\sum_{n=1}^{\infty}x_n^2 < \infty$converges. From the proceeding $x_n \in \xi^1 \Leftrightarrow x_n \in \xi^2$i.e. $\xi^1 \subseteq \xi^2$. Further, if$x_n = \frac{1}{n^{\frac{3}{4}}}$, then $\sum_{n=1}^{\infty}|x_n|$diverges and thus$x_n \notin \xi^1$. But $\sum_{n=1}^{\infty}x_n^2 = \sum_{n=1}^{\infty}\frac{1}{n^{\frac{3}{4}}}$converges, implying that$x_n \in \xi^2$. We conclude that $\xi^1 \subseteq \xi^2$and thus$\xi^1 \neq \xi^2$. If $(x_n, y_n)$are sequences of real numbers, then;

$\sum_{n=1}^{\infty}(x_i - y_i)^2 \leq \sum_{n=1}^{\infty}{x_i}^2 + \sum_{n=1}^{\infty}{y_i}^2 + 2[\sum_{n=1}^{\infty}{x_i}^2]^{\frac{1}{2}}[\sum_{n=1}^{\infty}{y_i}^2]^{\frac{1}{2}}$ (12)

Therefore if $\sum_{n=1}^{\infty}{x_i}^2 < \infty$and $\sum_{n=1}^{\infty}{y_i}^2 < \infty$then $\sum_{n=1}^{\infty}(x_i - y_i)^2 < \infty$for all n. The monotone increasing sequence $[\sum_{n=1}^{\infty}(x_i - y_i)^2]$is then bounded above and hence converges i.e. $\sum_{n=1}^{\infty}(x_i - y_i)^2 < \infty$. Thus $(x_i - y_i)^2 \in \xi^2$if $(x_n, y_n) \in \xi^2$.

Consequently, considering the compartmental disposition.

$\Gamma = \left((S(t), E(t), I(t), T(t), R(t), V(t) \in \Re_6^+ : N(t)\frac{\mu}{\varphi}\right)$ (13)

it is obtained as;

$\frac{dS}{dt} = \mu N - \beta\frac{I}{N}S - (\alpha + \rho + \varphi)S$

$\frac{dS}{dt} \geq -\beta\frac{I}{N}S - (\alpha + \rho + \varphi)S$

$\frac{dS}{S(t)} \geq -(\beta + \alpha + \rho + \varphi)dt$ (14)

$\int\frac{dS}{S(t)} \geq -\int(\beta + \alpha + \rho + \varphi)dt$

$InS(t) \geq -(\beta + \alpha + \rho + \varphi)dt$

$S(t) \geq S_0\ell^{-(\beta+\alpha+\rho+\varphi)t} > 0$

At $t > 0$,$S(t) > 0$

In the second compartment as deduced from the disease free equilibrium, it is obtained for E(t), I(t) and R(t).

$\frac{dE}{dt} = \beta\frac{I}{N}S - (\sigma + \varphi)E$

$\frac{dE}{dt} \geq -(\sigma + \varphi)E$

$\frac{dS}{E(t)} \geq -(\sigma + \varphi)dt$ (15)

$\int\frac{dE}{E(t)} \geq -\int(\sigma + \varphi)dt$

$InE(t) \geq -(\sigma + \varphi)dt$

$E(t) \geq E_0\ell^{-(\sigma+\varphi)t} > 0$

At $t > 0$,$E(t) > 0$

Thirdly,

$\frac{dI}{dt} = \sigma E - (\gamma_1 + \delta + \theta + \varphi)I$ (16)

$\frac{dI}{dt} \geq -(\gamma_1 + \delta + \theta + \varphi)I$

$\frac{dI}{I(t)} \geq -(\gamma_1 + \delta + \theta + \varphi)dt$

$\int\frac{dI}{I(t)} \geq -\int(\gamma_1 + \delta + \theta + \varphi)dt$

$InI(t) \geq -(\gamma_1 + \delta + \theta + \varphi)dt$

$I(t) \geq I_0\ell^{-(\gamma_1+\delta+\theta+\varphi)t} > 0$

At $t > 0$,$I(t) > 0$

Also,

$\frac{dT}{dt} = \rho S + \delta I - (\gamma_2 + \varphi)T$

$\frac{dT}{dt} \geq -(\gamma_2 + \varphi)T$

$\frac{dT}{T(t)} \geq -(\gamma_2 + \varphi)dt$ (17)

$\int\frac{dT}{T(t)} \geq -\int(\gamma_2 + \varphi)dt$

$InT(t) \geq -(\gamma_2 + \varphi)dt$

$T(t) \geq T_0\ell^{-(\gamma_2+\varphi)t} > 0$

At $t > 0$,$T(t) > 0$

$\frac{dR}{dt} = (\theta + \gamma_1)I + \gamma_2 T - (\varphi + \omega)R$

$\frac{dR}{dt} \geq -(\varphi + \omega)R$

$\frac{dR}{R(t)} \geq -(\varphi + \omega)dt$ (18)

$$\int \frac{dR}{R(t)} \geq -\int (\varphi+\omega)dt$$
$$InR(t) \geq -(\varphi+\omega)dt$$
$$R(t) \geq R_0 \ell^{-(\varphi+\omega)(t} > 0$$
At $t > 0, R(t) > 0$
$$\frac{dV}{dt} = \alpha S - (\varphi+\eta)V$$
$$\frac{dV}{dt} \geq -(\varphi+\eta)I$$
$$\frac{dV}{V(t)} \geq -(\varphi+\eta)dt \quad (19)$$
$$\int \frac{dV}{V(t)} \geq -\int (\varphi+\eta)dt$$
$$InV(t) \geq -(\varphi+\eta)dt$$
$$V(t) \geq V_0 \ell^{-(\varphi+\eta)t} > 0$$
At $t > 0, V(t) > 0$

Equation (14) to (19) shows system (1) in the positive quadrant, persisting in the attracting subsetΓ, which is compact, positively invariant, and influential, with a well-posed, epidemiologically and mathematically represented solution.

Disease Free Equilibrium State

The equilibrium state of non-infected individuals with measles signifies a system devoid of measles, encompassing individuals categorized as infected (I) and exposed (E)$I = E = 0$.

$$N^{\bullet} = S^{\bullet} + E^{\bullet} + I^{\bullet} + T^{\bullet} + R^{\bullet} + V^{\bullet} = 0 \quad (20)$$
$$\mu N - \beta \frac{I}{N} S - (\alpha+\rho+\varphi)S = 0$$
$$\beta \frac{I}{N} S - (\sigma+\varphi)E = 0$$
$$\sigma E - (\gamma_1+\delta+\theta+\varphi)I = 0$$
$$\rho S + \delta I - (\gamma_2+\varphi)T = 0$$
$$(\gamma_1+\theta)I + \gamma_2 T - \varphi R = 0$$
$$\alpha S - \varphi V = 0$$

When measles is of no spread, the disease classes are subjected $I = E = 0$are considered at equilibrium where

$\mu N - \beta \frac{I}{N} S - (\alpha+\rho+\varphi)S = 0$, $S = \frac{\mu}{(\alpha+\rho+\varphi)}$,

$T = \frac{\rho\mu}{(\alpha+\rho+\varphi)(\gamma_2+\varphi)}$,

$R = \frac{\rho\mu\gamma_2}{\varphi(\alpha+\rho+\varphi)(\gamma_2+\varphi)}$and $V = \frac{\alpha\mu}{(\alpha+\rho+\varphi)}$

Thus, the disease-free equilibrium yields:

$$(S_0, E_0, I_0, T_0, R, V_0) = \left(\frac{\mu}{(\alpha+\rho+\varphi)}, 0, 0, \frac{\rho\mu}{(\alpha+\rho+\varphi)(\gamma_2+\varphi)}, \frac{\rho\mu\gamma_2}{\varphi(\alpha+\rho+\varphi)(\gamma_2+\varphi)}, \frac{\alpha\mu}{(\alpha+\rho+\varphi)}\right) \quad (21)$$

Steady State Prevalence

It is crucial to highlight the dynamic nature of measles prevalence, especially its central role in sustaining outbreaks within a population. To analyze the system at equilibrium, consider the set of equations in (1), where the equilibrium points represent the endemic states of measles prevalence. $\Phi = (S^{\bullet}, E^{\bullet}, I^{\bullet}, R^{\bullet})$and $t > 0$

$$\alpha S - \varphi V = 0$$
$$S^* = \frac{\beta\mu\alpha\mu + (\alpha+\rho+\varphi)}{\alpha^2(\alpha+\rho+\varphi)+(\alpha+\rho+\varphi)}, \; E^* = \frac{\beta^2\mu\alpha\mu + (\alpha+\rho+\varphi)}{\alpha(\sigma+\varphi)(\alpha+\rho+\varphi)^2+(\alpha+\rho+\varphi)}$$
$$I^{\bullet} = \frac{\beta^2\sigma\mu\alpha\mu + (\alpha+\rho+\varphi)}{(\gamma_1+\delta+\theta+\varphi)[\alpha(\sigma+\varphi)(\alpha+\rho+\varphi)^2+(\alpha+\rho+\varphi)]} \quad (22)$$
$$T^* = \frac{1}{(\gamma_2+\phi)}\left(\frac{\beta\mu\alpha\mu + (\alpha+\rho+\phi)}{\alpha^2(\alpha+\rho+\phi)+(\alpha+\rho+\phi)} + \frac{\beta^2\sigma\mu\alpha\mu + (\alpha+\rho+\phi)}{(\gamma_1+\delta+\phi)[\alpha(\sigma+\phi)(\alpha+\rho+\phi)^2+(\alpha+\rho+\phi)]}\right)$$
$$R^* = \frac{(\gamma_2+\varphi)[\beta\mu\alpha\mu + (\alpha+\rho+\varphi) + \beta^2\sigma\mu\alpha\mu + (\alpha+\rho+\varphi)}{\alpha^2[(\alpha+\rho+\varphi)+(\alpha+\rho+\theta+\varphi)+(\gamma_1+\delta+\varphi)]^2[\alpha(\sigma+\varphi)(\alpha+\theta+\rho+\varphi)^2+(\alpha+\rho+\varphi)]}$$
$$S^* = \frac{\beta\alpha\mu\alpha\mu + (\alpha+\rho+\varphi)}{\alpha^2\varphi(\alpha+\rho+\varphi)+(\alpha+\rho+\varphi)}$$

The Disease Threshold R_0

The basic reproduction number, denoted asR_0. To quantify the likelihood of new measles infections arising from a single infectious individual in a previously unexposed population, we apply the next-generation matrix approach to construct the system outlined in (1), with a focus on infectious compartments. In this method, the $F$and V matrices are computed, representing the rate of new infections and the rate of transitions into and out of the infected compartment, respectively. This approach captures the dynamics of measles transmission and reinfection, emphasizing the importance of treatment as a critical control measure. These matrices are obtained using a complex derivation from the equations in System (1),$R_0 = \rho(G - \lambda I)$ taking $G = F \times V^{-1}$and $\rho$is the spectral radius of the matrix $|G - \lambda I|$.From the system of equation (1) it is obtained for matrix $F$and$V$: $F_i = \left(\frac{\partial f_i(x_i)}{\partial x_j}\right) V_i = \left(\frac{\partial v_i(x_i)}{\partial x_j}\right)$ (23)

and such that

$$f = \begin{pmatrix} \frac{\beta I S_0}{N} \\ 0 \end{pmatrix} \text{and} v = \begin{pmatrix} (\sigma+\varphi)E \\ -\sigma E + (\gamma_1+\theta+\delta+\varphi)I \end{pmatrix} \quad (24)$$

then,

$$F = \left(\frac{\beta\mu}{(\alpha+\rho+\varphi)}\right) V = \begin{pmatrix} (\sigma+\varphi) & 0 \\ \sigma & (\gamma_1+\theta+\delta+\varphi) \end{pmatrix}$$
$$FV^{-1} = \frac{1}{(\alpha+\rho+\varphi)(\sigma+\varphi)} \begin{pmatrix} \frac{\beta\mu}{(\alpha+\rho+\varphi)} & 0 \\ 0 & 0 \end{pmatrix} \begin{pmatrix} (\sigma+\varphi) & 0 \\ \sigma & (\gamma_1+\theta+\delta+\varphi) \end{pmatrix}$$
$$R_0 = \frac{\beta\mu(\sigma+\varphi)}{\mu(\alpha+\rho+\varphi)(\gamma_1+\theta+\delta+\varphi)(\sigma+\varphi)} \quad (25)$$

It results that the basic reproductive ratio determines the number of infected individual migrating to the subpopulation of exposed and infected, as this affect the level of recovery form the spread of measles. The leading eigenvalue of the non-invariant is the basic reproduction number of the disease model

Local Stability of the Disease-Free State

We examined the local stability of the disease-free state for measles by analysing the minimal recurrence rate impact. When the recurrence rate$R_* < 1$, the disease declines, to determine stability using a Jacobian matrix and a characteristic equation.

Lemma 1

The disease-free state of the model is locally asymptotically stable$R_* < 1$, otherwise $R_* > 1$if and only if the disease state prevails.

Proof:

The disease-free equilibrium obtained as the Jacobian matrix of the system of (1) is evaluated at the disease free State using the linearization thus;

$$J_{E_0} = \begin{pmatrix} -\frac{\mu}{(\alpha+\rho+\varphi)} & 0 & -\frac{\mu}{(\alpha+\rho+\varphi)} & 0 & 0 & 0 \\ \frac{\mu}{(\alpha+\rho+\varphi)} & -(\sigma+\varphi) & 0 & 0 & 0 & 0 \\ 0 & \sigma & -(\gamma_1+\theta+\delta+\varphi) & 0 & 0 & 0 \\ \rho & 0 & \delta & -(\gamma_2+\varphi) & 0 & 0 \\ 0 & 0 & \gamma_1 & \gamma_2 & -\varphi & 0 \\ \alpha & 0 & 0 & 0 & 0 & -\varphi \end{pmatrix}$$

$$\begin{pmatrix} -\frac{\mu}{(\alpha+\rho+\varphi)} & 0 & -\frac{\mu}{(\alpha+\rho+\varphi)} & 0 & 0 & 0 \\ \frac{\mu}{(\alpha+\rho+\varphi)} & -(\sigma+\varphi) & 0 & 0 & 0 & 0 \\ 0 & \sigma & -(\gamma_1+\theta+\delta+\varphi) & 0 & 0 & 0 \\ \rho & 0 & \delta & -(\gamma_2+\varphi) & 0 & 0 \\ 0 & 0 & \gamma_1 & \gamma_2 & -\varphi & 0 \\ \alpha & 0 & 0 & 0 & 0 & -\varphi \end{pmatrix} - \lambda \begin{pmatrix} 10 & 0 & 0 & 0 & 0 & 0 \\ 0 & 1 & 0 & 0 & 0 & 0 \\ 0 & 0 & 1 & 0 & 0 & 0 \\ 0 & 0 & 0 & 1 & 0 & 0 \\ 0 & 0 & 0 & 0 & 1 & 0 \\ 0 & 0 & 0 & 0 & 0 & 1 \end{pmatrix}$$

$$\begin{vmatrix} -\frac{\mu}{(\alpha+\rho+\varphi)} - \lambda_1 & 0 & -\frac{\mu}{(\alpha+\rho+\varphi)} & 0 & 0 & 0 \\ \frac{\mu}{(\alpha+\rho+\varphi)} & -(\sigma+\varphi)-\lambda_2 & 0 & 0 & 0 & 0 \\ 0 & \sigma & -(\gamma_1+\theta+\delta+\varphi)-\lambda_3 & 0 & 0 & 0 \\ \rho & 0 & \delta & -(\gamma_2+\varphi)-\lambda_4 & 0 & 0 \\ 0 & 0 & \gamma_1 & \gamma_2 & -\varphi-\lambda_5 & 0 \\ \alpha & 0 & 0 & 0 & 0 & -\varphi-\lambda_6 \end{vmatrix} = 0$$

Computing for the eigenvalues,$\left|J_{E_1} - \lambda_i I\right| = 0$, from the Jacobian matrix the respective eigen values of the matrix can be obtained as;

$$\begin{vmatrix} -\varphi-\lambda_5 & 0 \\ 0 & -\varphi-\lambda_6 \end{vmatrix} = 0 \quad \lambda_5 = \lambda_6 = -\varphi$$

$$(A-\lambda_1)(B-\lambda_2)(C-\lambda_3)(D-\lambda_4)(E-\lambda_5)(A-\lambda_6) = 0 \tag{26}$$

The negativity of the invariants region with respective eigen values obtained for the model equation is asymptotically stable.

Local stability of endemic equilibrium point

Lemma 2

The regional resilience of the persistent equilibrium of the proposed model is locally asymptotically stable if and unstable otherwise if $R_* > 1$

Proof:

Suppose,$S = x + S^*, E = y + E^*, I = z + I^*, T = a + T^*, R = b + R^*, V = c + V^*$ (27)

Linearizing equation (1), is then obtained as

$$J_{E_0} = \begin{pmatrix} -\frac{\mu}{(\alpha+\rho+\varphi)} & 0 & -\frac{\mu}{(\alpha+\rho+\varphi)} & 0 & 0 & 0 \\ \frac{\mu}{(\alpha+\rho+\varphi)} & -(\sigma+\varphi) & 0 & 0 & 0 & 0 \\ 0 & \sigma & -(\gamma_1+\theta+\delta+\varphi) & 0 & 0 & 0 \\ \rho & 0 & \delta & -(\gamma_2+\varphi) & 0 & 0 \\ 0 & 0 & \gamma_1 & \gamma_2 & -\varphi & 0 \\ \alpha & 0 & 0 & 0 & 0 & -\varphi \end{pmatrix}$$

$$\mu N - \beta \frac{I}{N} S - (\alpha+\rho+\varphi)S = 0$$

$$\left.\begin{aligned} \frac{dx}{dt} &= -\beta xz(\rho+\alpha+\varphi) - \mu x + \text{higher order } + \text{ nonlinear terms...} \\ \frac{dy}{dt} &= \beta xz(a+\alpha c)^{-1} - (\mu+\varphi+\rho)y + \text{higher order } + \text{ nonlinear terms...} \\ \frac{dz}{dt} &= \sigma y + (+\theta+\gamma_1+\varphi)z - \gamma_2 z + \delta a + \text{higher order } + \text{ nonlinear terms...} \\ \frac{da}{dt} &= \rho z + \delta c - (\rho+\delta+\varphi)a + \text{higher order } + \text{ nonlinear terms...} \\ \frac{db}{dt} &= (\gamma_2+\varphi+)a + \rho b + \text{higher order } + \text{ nonlinear terms...} \\ \frac{dc}{dt} &= \alpha z - \varphi c + \text{higher order } + \text{ nonlinear terms...} \end{aligned}\right\} \tag{28}$$

Jacobian matrix of the system of

$$\begin{vmatrix} -(2\beta(1+\alpha)^{-1}+\varphi) & 0 & (2\beta(1+\alpha)^{-1}+\varphi) & 0 \\ (2\beta(1+\alpha)^{-1}+\varphi) & -(\delta+\gamma_1+\varphi) & 2\beta(1+\alpha)^{-1}+(\delta+\gamma+\varphi) & 0 \\ 0 & \delta & -(\delta+\gamma_2+\varphi) & 0 \\ 0 & 0 & (\varphi+\rho+\delta) & -(\rho+\delta+\varphi) \end{vmatrix} = 0$$

The resulting eigenvalue of the above matrix is obtained as;

$(-(2\beta(1+\alpha)^{-1}+\varphi)-\lambda_1)(-(\delta+\gamma_1+\varphi)-\lambda_2)(-(\rho+\gamma_2+\varphi)-\lambda_3)(-(\delta+\varphi)-\lambda_4)(-(2\beta(\delta+\alpha)^{-1}+\varphi)-\lambda_5)$
$(-(2\beta(\rho+\alpha)^{-1}+\varphi)-\lambda_6)=0$ (35)

If $a=-(2\beta(1+\alpha)^{-1}, b=-(\varepsilon+\mu), c=-(T+\gamma+\mu), d=-(\delta+\mu)$ (29)

It is therefore obtained that

$(a-\lambda_1)(b-\lambda_2)(c-\lambda_3)(d-\lambda_4)(e-\lambda_5)(f-\lambda_6)=0$
$\lambda^6-[(a+b+d)(c+f+f)+ab+cd]+\lambda^5[(a+e)(b+d)+ef+cd]-[abd(c+b)+ae(c+e)]\lambda^3$
$[bef(a+b)+bc(a+b+d)]\lambda^3+[ae+ad+bd+ac]\lambda^2+[(e+a)+(b+c)]\lambda+abcdef=0$

Therefore, the persistent resilience of the respective Eigen values in the model invariance region of $\Re_4^+$ is asymptotically stable.

Global Stability of Disease Free Equilibrium

Employing Lyapunov function approach, we establish the global asymptotic stability of the proposed model for equation (1) at the disease-free equilibrium, utilizing the Lyapunov algorithm.

$\Psi(t,S,E,I,T,R,V)=C_1I_1+C_2I_2$
$(S_0,E_0,I_0,T_0,R,V_0)=\left(\frac{\mu}{(\alpha+\rho+\varphi)},0,0,\frac{\rho\mu}{(\alpha+\rho+\varphi)(\gamma_2+\varphi)},\frac{\rho\mu\gamma_2}{\varphi(\alpha+\rho+\varphi)(\gamma_2+\varphi)},\frac{\alpha\mu}{(\alpha+\rho+\varphi)}\right)$ (30)
$\frac{d\Psi}{dt}=C_1I_1^{\bullet}+C_2I_2^{\bullet}=C_1\left(\frac{\beta\alpha}{(\alpha+\rho+\varphi)}-(\mu+\delta+\varphi)I_1\right)+C_2(\sigma I_1-(\mu+\gamma_1+\varphi)]I_2)$
$\frac{d\Psi}{dt}\leq(C_2\sigma-C_1(\mu+\delta+\varphi))I_1-\left(C_1\frac{\beta\alpha}{(\alpha+\rho+\varphi)}-C_2(\mu+\gamma+\varphi)\right)I_2$
$\frac{d\Psi}{dt}\leq C_1(C_2\sigma-C_1(\mu+\varphi+\gamma_1))I_1-\left(C_2\frac{\beta\alpha}{(\alpha+\rho+\varphi)}-C_2(\mu+\gamma+\varphi)\right)I_2$
$C_1=\frac{1}{(\alpha+\varphi+\gamma_1)}, C_2=\frac{\beta\alpha\varphi}{\mu(\delta+\varphi+\gamma_1)(\alpha+\varphi+\gamma_2)(\alpha+\varphi+\gamma_1)}, R\leq 0$
$\frac{d\Psi}{dt}\leq C_1\left(\frac{\beta\mu(\sigma+\varphi)}{\mu(\alpha+\rho+\varphi)(\gamma_1+\delta+\varphi)(\sigma+\varphi)}-\frac{(\alpha+\varphi+\gamma_1)}{(\alpha+\varphi+\gamma_1)}\right)I_1$
$-\left(\frac{\beta\alpha\varphi}{\mu(\delta+\varphi+\gamma_1)(\alpha+\varphi+\gamma_2)(\alpha+\varphi+\gamma_1)}-\frac{\beta\alpha\varphi}{\mu(\delta+\varphi+\gamma_1)(\alpha+\varphi+\gamma_2)(\alpha+\varphi+\gamma_1)}\right)I_2$
$\frac{d\Psi}{dt}\leq\left(\frac{\beta\mu(\sigma+\varphi)}{\mu(\alpha+\rho+\varphi)(\gamma_1+\delta+\varphi)(\sigma+\varphi)}-1\right)I$
$\frac{d\Psi}{dt}\leq(R_0-1)$ (31)

It is pertinent that when at $t\longrightarrow\infty, \frac{d\psi}{dt}\leq 0$. Substituting into the model system of equation (1) reveals that, based on LaSalle's invariance principle$\frac{d\psi}{dt}=0$, is globally asymptotically stable whenever $R_0>1$

Global stability for endemic equilibrium

Theorem 3

The Dulac criterion provides a technique in dynamical systems for proving the non-resistance of periodic orbits within a specified region of the phase plane. In the context of a mathematical model of measles, this criterion can be extended to examine the global stability of an equilibrium point, confirming that recurrent measles outbreaks cannot persist under the given model conditions.

Proof:

For a dynamical system described by the differential equations:

$\frac{dx}{dt}=f(x,y)\Leftrightarrow\frac{dy}{dt}=g(x,y)$ (32)

The Dulac criterion states that if there exists a continuously differentiable function $B(x,y)$ (called the Dulac function) such that the expression:

$\frac{\partial}{\partial x}(B(x,y)f(x,y))+\frac{\partial}{\partial x}(B(x,y)g(x,y))$ (33)

is either strictly positive or strictly negative throughout a simply connected region$D$ of the phase plane, then there are no closed trajectories (periodic orbits) contained entirely within D.

To apply this to determine the global stability of an endemic equilibrium $(x^*,y^*)$of a mathematical model, the endemic equilibrium point(x^*,y^*). Also define the Dulac function $B(x,y)$and the expression $\frac{\partial}{\partial x}(B(x,y)f(x,y))+\frac{\partial}{\partial x}(B(x,y)g(x,y))$ as $B(x,y)g(x,y)$ (34)

This shows that this expression is of one sign (either strictly positive or strictly negative) in the region of interest. If such a Dulac function $B(x,y)$ can be found, the system has no periodic orbits in that region, suggesting the global stability of the endemic equilibrium if no other attractors exist. Hence, if $\exists B(x,y)\in C^1$such that $\frac{\partial}{\partial x}(B(x,y)f(x,y))+\frac{\partial}{\partial x}(B(x,y)g(x,y))\neq 0inD$. Then there are no closed trajectories in D.This criterion is useful in proving the global stability of the endemic equilibrium when combined with other stability analysis techniques.

We employ this concept of Dulac's criterion. Let $X=(S,E,I,T,R,V)$define the Dulac's function $G=\frac{1}{SI}$. The following system of equation are obtained;

$$G\frac{dS}{dt}=\frac{1}{SI}\left\{\mu N-\beta\frac{I}{N}S-(\alpha+\rho+\varphi)S\right\}$$
$$G\frac{dE}{dt}=\frac{1}{SI}\left\{\beta\frac{I}{N}S-(\sigma+\varphi)E\right\}$$
$$G\frac{dI}{dt}=\frac{1}{SI}\{\sigma E-(\gamma_1+\delta+\varphi)I\} \quad (35)$$
$$G\frac{dT}{dt}=\frac{1}{SI}\{\rho S+\delta I-(\gamma_2+\varphi)T\}$$
$$G\frac{dR}{dt}=\frac{1}{SI}\{\gamma_1 I+\gamma_2 T-\varphi+\omega R\}$$
$$G\frac{dV}{dt}=\frac{1}{SI}\{\alpha S-\varphi+\eta V\}$$

The above system of equations results to;

$$G\frac{dS}{dt}=\left\{\frac{\mu N}{SI}-\frac{\beta I}{I}-\frac{(\alpha+\rho+\varphi)}{I}\right\}\text{c}$$
$$G\frac{dE}{dt}=\left\{\frac{\beta}{N}-\frac{\beta(\sigma+\varphi)E}{SI}\right\}$$
$$G\frac{dI}{dt}=\left\{\frac{\sigma E}{SI}-\frac{\sigma E(\gamma_1+\delta+\varphi)}{S}\right\}$$
$$G\frac{dT}{dt}=\left\{\frac{\rho}{I}+\frac{\delta}{S}-\frac{(\gamma_2+\varphi)}{SI}\right\}$$
$$G\frac{dR}{dt}=\frac{1}{SI}\left\{\frac{\gamma_1}{S}+\frac{\gamma_2 T}{S}-\frac{\varphi R}{S}\right\}$$
$$G\frac{dV}{dt}=\left\{\frac{\alpha}{I}-\frac{\varphi+\eta V}{SI}\right\}$$

At $t>0$ orbital resolution of the system of equations is given by $\frac{d(GX)}{dt}$ as obtained below.

$$\frac{d(GX)}{dt}=\frac{\partial}{\partial S}\left\{G\frac{dS}{dt}\right\}+\frac{\partial}{\partial E}\left\{G\frac{dE}{dt}\right\}+\frac{\partial}{\partial I}\left\{G\frac{dI}{dt}\right\}+\frac{\partial}{\partial R}\left\{G\frac{dR}{dt}\right\}$$
$$\frac{d(GX)}{dt}=\frac{\partial}{\partial S}\left\{\frac{\Lambda}{SI}-\frac{\beta}{(\varphi+\alpha+\delta)}-\frac{\mu}{I}\right\}+\frac{\partial}{\partial E}\left\{\frac{\beta}{(\varphi+\theta+\alpha+\gamma_1)}-\frac{(\mu+\varepsilon)E}{SI}\right\}+\frac{\partial}{\partial I}\left\{\frac{\varepsilon E}{SI}-\frac{(\varphi+\alpha+\gamma_2)}{S}+\frac{\delta R}{SI}\right\}+\frac{\partial}{\partial T}\left\{\frac{T}{SI}+\frac{\gamma}{S}-\frac{(\mu+\delta)R}{SI}\right\}+\frac{\partial}{\partial R}\left\{\frac{T}{SI}+\frac{\gamma}{S}-\frac{(\sigma+\varphi+\delta)R}{SI}\right\}+\frac{\partial}{\partial V}\left\{+\frac{\varphi}{S}-\frac{(\mu+\varphi)R}{SI}\right\}$$
$$\frac{d(GX)}{dt}=\frac{\partial}{\partial S}\left\{\frac{\Lambda}{SI}-\frac{\beta}{(\phi+\alpha+\delta)}-\frac{\mu}{I}\right\}+\frac{\partial}{\partial E}\left\{\frac{\beta}{(\phi+\alpha+\theta+\gamma_1)}-\frac{(\mu+\varepsilon)E}{SI}\right\}+\frac{\partial}{\partial I}\left\{\frac{\varepsilon E}{SI}-\frac{(\phi+\alpha+\gamma_2)}{S}+\frac{\delta R}{SI}\right\}$$
$$+\frac{\partial}{\partial T}\left\{\frac{T}{SI}+\frac{\gamma}{S}-\frac{(\mu+\delta)R}{SI}\right\}+\frac{\partial}{\partial R}\left\{\frac{T}{SI}+\frac{\gamma}{S}-\frac{(\sigma+\phi+\delta)R}{SI}\right\}+\frac{\partial}{\partial V}\left\{+\frac{\phi}{S}-\frac{(\mu+\phi)R}{SI}\right\}$$
$$\frac{d(GX)}{dt}=-\left\{\begin{matrix}\frac{[(\beta+\alpha+\delta)+\beta+\varphi(\gamma_1+\alpha+\varphi)]}{(\delta+\varphi+\alpha)}+\frac{[\beta+(\mu+\varepsilon)]}{S(\varphi+\alpha)}\\+\frac{[(\gamma_1+\theta+\delta+\varphi)]}{SI}+\frac{[(\gamma_2+\alpha+\varphi)]}{SI}\end{matrix}\right\} \quad (36)$$
$$\frac{d(GX)}{dt}=-\left\{\frac{\beta(\beta+\alpha+\delta)+\beta+\varphi(\gamma_2+\alpha+\varphi)+[(\gamma_1+\theta+\alpha+\delta)+\beta+\varphi(\gamma_2+\alpha+\varphi)]}{SI}\right\}<0$$

This result indicates that the system lacks closed orbits, meaning there are no periodic fluctuations in the number of infected individuals. Epidemiologically, this suggests that sustained oscillations in measles cases do not occur, underscoring the importance of treatment as a primary control strategy. By focusing on measles treatment, resource allocation can be optimized to effectively reduce and eventually halt the rapid spread of the disease with time.

Sensitivity Analysis of R_0

The primary aim is to assess the sensitivity of the basic reproduction number, by computing its derivative concerning all relevant parameters. This analysis will result in the determination of the normalized forward sensitivity index, denoted as

$$R_0=\frac{\beta\mu(\sigma+\varphi)}{\mu(\alpha+\rho+\varphi)(\gamma_1+\delta+\varphi)(\sigma+\varphi)}$$
$$\frac{\partial R_0}{\partial\beta}=\frac{\partial R_0}{\partial\beta}\times\frac{\beta}{R_0}=0.01206000\quad\frac{\partial R_0}{\partial\mu}=\frac{\partial R_0}{\partial\mu}\times\frac{\mu}{R_0}=0.00130200$$
$$\frac{\partial R_0}{\partial\rho}=\frac{\partial R_0}{\partial\rho}\times\frac{\rho}{R_0}=1.03267370\quad\frac{\partial R_0}{\partial\sigma}=\frac{\partial R_0}{\partial\sigma}\times\frac{\sigma}{R_0}=0.00130 \quad (37)$$
$$\frac{\partial R_0}{\partial\gamma_1}=\frac{\partial R_0}{\partial\gamma_1}\times\frac{\gamma_1}{R_0}=0.1874342\quad\frac{\partial R_0}{\partial\varphi}=\frac{\partial R_0}{\partial\varphi}\times\frac{\varphi}{R_0}=0.15356728$$
$$\frac{\partial R_0}{\partial\gamma_2}=\frac{\partial R_0}{\partial\gamma_2}\times\frac{\gamma_2}{R_0}=0.1227361\quad\frac{\partial R_0}{\partial N}=\frac{\partial R_0}{\partial N}\times\frac{N}{R_0}=1.00000000$$
$$\frac{\partial R_0}{\partial\delta}=\frac{\partial R_0}{\partial\delta}\times\frac{\delta}{R_0}=0.00000040$$

Table 3: Sensitivity Analysis and Parameter Indices

Parameters	Sensitivity indices
β	0.07362
μ	1.28373
α	0.03421
γ_2	0.00125
δ	1.10932
γ_1	1.90243
σ	0.59824
φ	0.19232

Table 3 shows that the sensitivity indices of are positively invariant in $\Re_5^+$ the sensitivity indices depend on the values of the each parameters ofR_0, and this brings about changes in the values that will affect the behaviour of the threshold on the spread or vanity of measles disease. Based on the table, we can conclude that parameters are the most sensitive to the basic reproduction number in equation (18) of the measles model. Particularly, increasing the value of σ will result in a 96.96% increase inR_*, while increasing the value of $k$will lead to a 91.52% decrease in R_0.

Numerical Simulation

Homotopy Perturbation Method (HPM) is an elegant and powerful method to solve linear and non-linear partial differential equations. As we know to get an exact solution of non- linear partial differential equation is very difficult, so any kind of perturbative approach is acceptable depending on its criteria. HPM provides an analytical solution by using the initial conditions. It is interesting to note that only a few terms are required to obtain a most accurate approximate solution. This section, we have illustrated the basic idea of homotopy perturbation method to apply in non-linear equations. Consider the following non-linear differential equation of the form.

$$A(u) - f(r) = 0, r \in \Omega \quad (38)$$

Subject to the boundary conditions:

$$B = \left(u, \frac{\partial u}{\partial n}\right) = 0, r \in \Gamma, \quad (39)$$

Where A is a general differential operator, B is a boundary operator, f(r) a known analytical function and Γis the boundary of the domainΩ. In general, one can divide the operation A into two parts: Linear and non-linear. That means $A = L + N$

Where L is Linear and N is the non-linear,

Hence, equation (3) can now be rewritten as

$$L(u) + N(u) + f(r) = 0, r \in \Omega \quad (40)$$

By the homotopy technique, one can construct a homotopy in the following way

$v(r,p): \Omega \times [0,1] \to R$ This satisfies

$$H(V,P) = (1-P)[L(v) - L(u_0)] + P[A(v) - f(r) = 0, P \in [0,1], r \in \Omega \quad (41)$$

Constructing a homotopy perturbation method using an algorithm developed on each compartment of the model. We conduct the numerical simulation on the mathematical model using the concept of homotopy perturbation method which brings about creating the following correctional scheme for the model equation.

The differential equation of the model formulation on the use of homotopy perturbation method technique is illustrated as;

$$(1-p)\frac{dS}{dt} + p\left(\frac{dS}{dt} - [\mu N - \beta\frac{I}{N}S - (\alpha+\rho+\varphi)S]\right) = 0$$

$$(1-p)\frac{dE}{dt} + p\left(\frac{dE}{dt} - [\frac{\beta SI}{1+\alpha I} - \beta\frac{I}{N}S - (\sigma+\varphi)E]\right) = 0$$

$$(1-p)\frac{dI}{dt} + p\left(\frac{dI}{dt} - [\varepsilon E - (\gamma_1+\delta+\varphi)I]\right) \quad (42)$$

$$(1-p)\frac{dR}{dt} + p\left(\frac{dR}{dt} - [\rho S + \delta I - (\gamma_2+\varphi)T]\right) = 0$$

$$(1-p)\frac{dR}{dt} + p\left(\frac{dR}{dt} - [\gamma_1 I + \gamma_2 T - \varphi + \omega R]\right) = 0$$

$$(1-p)\frac{dR}{dt} + p\left(\frac{dR}{dt} - [\alpha S - \varphi + \eta V]\right) = 0$$

The following correctional series are assumed as solutions for (1) such that

$S(t) = \sum_{k=0}^{n} p^k s_k(t), E(t) = \sum_{k=0}^{n} p^k e_k(t), I(t) = \sum_{k=0}^{n} p^k i_k(t), T(t) = \sum_{k=0}^{n} p^k t_k(t), R(t) = \sum_{k=0}^{n} p^k r_k(t), V(t) = \sum_{k=0}^{n} p^k v_k(t)$

This series converges as p tends to in each of the iterations is subjected to the initial conditions as$t \to 1$. Evaluating (32) and comparing coefficients of p^n yields the following at $n = 1$

$$\frac{dS}{dt} = 0, \frac{dE_o}{dt} = 0, \frac{dI_o}{dt} = 0, \frac{dV_o}{dt} = 0, \frac{dR_o}{dt} = 0, \frac{dV_o}{dt} = 0 \quad (43)$$

Solving these equations using the initial constraints

$$\mu N - \beta\frac{I}{N}S - (\alpha+\rho+\varphi)S = 0$$
$$\beta\frac{I}{N}S - (\sigma+\varphi)E = 0$$
$$\sigma E - (\gamma_1+\delta+\varphi)I = 0$$
$$\rho S + \delta I - (\gamma_2+\varphi)T = 0$$
$$\gamma_1 I + \gamma_2 T - (\varphi+\omega)R = 0$$
$$\alpha S - (\varphi+\eta)V = 0$$

$S_0(t) = s_0, E_0(t) = e_0, I_0(t) = i_0, R_0(t) = r_0$, at this initial condition, the result obtained from (32) is deduced as

$$s(t) = (\mu N - \beta s_0 e_0 - (\alpha+\rho+\varphi) + s_0)t$$
$$e_1(t) = (\beta\alpha s_0 i_0 - (\sigma+\varphi)\alpha s_0 i_0 - \mu e_0 + \varepsilon e_0)t$$
$$i_1(t) = (\sigma e_0 - (\gamma_1+\delta+\varphi)\sigma e_0 - \mu i_0 - \delta i_0 - \rho i_0)t \quad (44)$$
$$t_1(t) = (\alpha e_0 i_0 - \mu r_0 - \beta i_0 + \varepsilon e_0)t$$
$$r_1(t) = (\gamma_1 + \gamma_2\alpha e - \varphi\alpha e_0 i_0 - \mu r_0 - \beta i_0 + \varepsilon e_0)t$$
$$v_1(t) = (\alpha - \varphi\alpha e_0 i_0 - \mu r_0 - \beta i_0 + \varepsilon e_0)t$$

The successive iterations of the results obtained at $n = 2$,

$$s_2(t) = \frac{1}{2}t^2\begin{pmatrix}\alpha^3 i^2{}_0 s_0 + \alpha^2\mu i_0 s_0 + \alpha^2\beta i_0 s_0 - \alpha^2\beta i_0 e_0 - \alpha^2{}_0 + \alpha\delta i_0 s_0 + 2\alpha\mu i_0 s_0 + \alpha\rho_0 s_0 - \alpha e_0 s_0 + \alpha\beta_{1_0} s_0 + \mu^2 s_0 \\ +2\mu\beta_1 s_0 - 2\mu\beta_1 r_0 - \beta_1{}^2 s_0 - \beta v_0 - \beta^2 v_0 - \mu\theta - \varepsilon\beta_1\end{pmatrix}$$

$$e_2(t) = -\frac{1}{2}t^2\begin{pmatrix}\alpha^2 i_0{}^2 s_0 + \alpha\delta i_0 s_0 + 3\alpha\mu i_0 s_0 + \alpha r_0 s_0 - \alpha i e_0 s_0 + \alpha e_{1_0} s_0 + \alpha\beta i_0 s_0 \\ -\alpha\beta i_0 s_0 - \alpha i_0 - \mu^2 e_0 - 2\mu e_0 - \gamma^2 e_0\end{pmatrix}$$

$$I_2(t) = -\frac{1}{2}t^2(\alpha\beta i_0 s_0 - \mu^2 T_0 + 2\mu T s_0 - 2\mu\beta v_0 + \beta^2 s_0 + \beta s_0 - \beta^2 v_0 - \mu\beta)$$

$$t_2(t) = -\frac{1}{2}t^2(\delta\rho i_0 - \mu^2 r_0 + 2\mu\varepsilon i_0 + \gamma^2 i_0 - \mu\varepsilon e_0)$$

$$r_2(t) = -\frac{1}{2}t^2(\delta\rho i_0 - \mu^2 r_0 + 2\mu\varepsilon i_0 + \gamma^2 i_0 - \mu\varepsilon e_0) \quad (45)$$

$$v_2(t) = -\frac{1}{3}t^2(\varphi\rho i_0 - \mu^2 e_0 - \mu\varepsilon e_0 + 2\gamma_2\gamma_1 e_0 r_0 - \delta\sigma\varepsilon e_0 + \gamma_1\beta\mu)$$

Subsequently, further iterations is carried out from the result of (52) at n = 3 results;

$$S_{3c}(t) =$$
$$-\frac{1}{6}t^3\begin{pmatrix} \mu^3 s_0 + +2\mu\beta_1 s_0 - 2\mu\beta_2 s_0 + \beta^2 s_0 + \beta_2\beta_1 s_0 - \beta v_0 - {\beta_2}^2 v_0\alpha^2\mu i_0 s_0 + \alpha^2\beta_1 i_0 s_0 - \alpha^2\beta_2 i_0 v_0 - \alpha^2\theta i_0 + \delta i_0 s_0 + \\ 2\alpha\mu i_0 s_0 + \alpha\rho_0 s_0 + 2\mu\beta_1 s_0 - 2\mu\beta_1 v_0 - {\beta_1}^2 s_0 + 5\beta_2\beta_1 s_0 - \beta_2\beta_1 v_0 - {\beta_2}^2 v_0 - \mu\theta - \theta\beta_1 - \alpha\sigma e_0 s_0 + \alpha\beta_{1_0} s_0 + \mu^2 s_0 + 3\mu\beta_1 s_0 \\ -2\mu\beta_1 v_0 - {\beta_1}^2 s_0 + 4\beta_2\beta_1 s_0 + +2\mu\beta_1 s_0 - 2\mu\beta_1 v_0 - {\beta_1}^2 s_0 + \beta_2\beta_1 s_0 - 5\beta_2\beta_1 v_0 - 3{\beta_2}^2 v_0 - \alpha i_0 s_0 - \mu s_0 - 3\beta_1 s_0 + 2\beta_2 v_0 + \theta - \mu\theta - \theta\beta \\ \&_1 - 2\beta_2\beta_1 v_0 - {\beta_2}^2 v_0 - \mu\theta - \theta\beta - 5\beta_1 s_0 - \beta_2 v_0 + \mu v_0 - 3\mu\beta_1 s_0 - 2\mu\beta_2 v_0 + {\beta_1}^2 s_0 + \beta_2\beta_1 s_0 - \beta_2\beta_1 v_{0\_} + \delta^2 i_0 + 2\delta\mu i_0 + 2\delta\rho i_0 - \delta\sigma e_0 + \mu^2 i_0 \\ +2\mu\rho i_{0_1} + 3\alpha\mu i_0 s_0 + \alpha\rho_0 s_0 - 3\alpha\sigma e_0 s_0 + \alpha\sigma_{1_0} s_0 + \alpha\beta_1 i_0 s_0 - \delta i_0 s_0 + 3\alpha\mu i_0 s_0 + \alpha\rho_0 s_0 - 2\alpha_0 s_0 + \alpha_{1_0} s_0 \end{pmatrix}$$

$$e_3(t)$$
$$= -\frac{1}{6}t^2\begin{pmatrix} {\alpha^2 i_0}^2 s_0 + \alpha\delta i_0 s_0 + 3\alpha\mu i_0 s_0 + \alpha\rho_0 s_0 - \alpha\sigma e_0 s_0 + \alpha\sigma_{1_0} s_0 + \alpha\beta_1 i_0 s_0 + 2\mu\beta_1 s_0 - 2\mu\beta_1 v_0 - {\beta_1}^2 s_0 + 5\beta_2\beta_1 s_0 - \beta_2\beta_1 v_0 - {\beta_2}^2 v_0 - \mu\theta \\ -\alpha\beta_2 i_0 v_0 - 3\alpha\theta i_0 - \mu^2 e_0 - 2\mu\sigma e_0 - \sigma^2 e_0 - \mu^2 r_0 + 2\mu\rho i_0 + \rho^2 i_0 + \alpha\beta_1 i_0 s_0 - 4\alpha\delta i_0 s_0 + 3\alpha\mu i_0 s_0 + \alpha\rho_0 s_0 - 2\alpha\sigma e_0 s + +\alpha\delta i_0 s_0 + 3\alpha\mu i_0 s_0 + \alpha\rho_0 s_0 \\ -\alpha\sigma e_0 s_0 + \alpha\sigma_{1_0} s_0 + \alpha\beta_{1_0} i_0 s_0 - \alpha\beta_2 i_0 v_0 - \alpha\theta i_0 - \mu^2 e_0 - 2\mu\sigma e_0 - \sigma^2 e_0 - \delta\rho i_0 - \mu^2 r_0 - 3\mu\beta_1 s_0 + {\beta_1}^2 s_0 + \beta_2\beta_1 s_0 - \beta_2\beta_1 v_0 - \beta_2{}^2 v_0 - \theta\beta_1 \\ + + \alpha\delta i_0 s_0\sigma e_0 - \mu i_0 - \delta i_0 - \rho i_0 + 2\mu\rho i_0 - 2\mu\sigma e_0 + \rho^2 i_0 - \rho\sigma e_0 - \sigma^2 e_0 \end{pmatrix}$$

$$I(t)$$
$$= -\frac{1}{6}t^2\begin{pmatrix} \alpha\sigma i_0 s_0 + \delta^2 i_0 + 2\delta\mu i_0 + 2\delta\rho i_0 - \delta\sigma e_0 + \mu^2 i_0 + 2\mu\rho i_0 - 2\mu\sigma e_0 + -\mu^2 r_0 + 2\mu\rho i_0 + \rho^2 i_0 + \alpha\beta_1 i_0 s_0 - 4\alpha\delta i_0 s_0 + 3\alpha\mu i_0 s_0 + \alpha\rho_0 s_0 - 2\alpha\sigma e_0 s \\ +\alpha\delta i_0 s_0 + 3\alpha\mu i_0 s_0 + \alpha\rho_0 s_0 - \alpha\sigma e_0 s_0 + \alpha\sigma_{1_0} s_0 + \rho^2 i_0 + -\beta_2{}^2 v_0 - \mu\theta - \theta\beta_1 - \alpha\sigma e_0 s_0 + \alpha\beta_{1_0} s_0 + \mu^2 s_0 + 3\mu\beta_1 s_0 - 2\mu\beta_1 v - \rho\sigma e_0 - \sigma^2 e_0 \\ +2\mu\rho i_0 + \rho^2 i_0 + \alpha\beta_1 i_0 s_0 - 4\alpha\delta i_0 s_0 + 3\alpha\mu i_0 s_0 + \alpha\rho_0 s_0 - 2\alpha\sigma e_0 s + +\alpha\delta i_0 s_0 + 3\alpha\mu i_0 s_0 + \alpha\rho_0 s_0 \\ -\alpha\sigma e_0 s_0 + \alpha\sigma_{1_0} s_0 + \alpha\beta_1 i_0 s_0 - \alpha\beta_2 i_0 v_0 - \alpha\theta i_0 - \mu^2 e_0 - 2\mu\sigma e_0 - \sigma^2 e_0 - \delta\rho i_0 \end{pmatrix}$$

$$t_3(t) = -\frac{1}{6}t^2\begin{pmatrix} \varphi\beta_1 i_0 s_0 - \alpha\beta_2 i_0 v_0 - \alpha\theta i_0 - \mu^2 e_0 - 2\mu\sigma - \varphi\sigma e_0 s_0 + \alpha\sigma_{1_0} s_0 + \alpha\beta_1 i_0 s_0 + 2\mu\beta_1 s_0 - \alpha\sigma e_0 s_0 \\ +\alpha\sigma_{1_0} s_0 + e_0 - \sigma^2 e_0 - \delta\rho i_0 - \mu^2 r_0\alpha\delta i_0 s_0\sigma e_0 - \mu i_0 - \rho\sigma e_0 - \sigma^2 e_0 \end{pmatrix}$$

$$r_2(t)$$
$$= -\frac{1}{6}t^2\begin{pmatrix} \delta\rho i_0 - \mu^2 r_0 + 2\mu\rho i_0 + \rho^2 i_0 + -\sigma^2 e_0 - \mu^2 r_0 + 2\mu\rho i_0 + \rho^2 i_0 + \alpha\beta_1 i_0 s_0 - 4\alpha\delta i_0 s_0 + 3\alpha\mu i_0 s_0 + \alpha\rho_0 s_0 - 2\alpha\sigma e_0 s + +\alpha\delta i_0 s_0 + 3\alpha\mu i_0 s_0 + \alpha\rho_0 s_0 \\ -\alpha\sigma e_0 s_0 + \alpha\sigma_{1_0} s_0 + \alpha\beta_1 i_0 s - \rho\sigma^2 e_0 \end{pmatrix}$$

$$v_2(t)$$
$$= -\frac{2}{3}t^2\begin{pmatrix} \delta\rho i_0 - \mu^2 r_0 + 2\mu\rho i_0 + \rho^2 i_0 + -\sigma^2 e_0 - \mu^2 r_0 + 2\mu\rho i_0 + \rho^2 i_0 + \alpha\beta_1 i_0 s_0 - 4\alpha\delta i_0 s_0 + 3\alpha\mu i_0 s_0 + \alpha\rho_0 s_0 - 2\alpha\sigma e_0 s + +\alpha\delta i_0 s_0 + 3\alpha\mu i_0 s_0 + \alpha\rho_0 s_0 \\ -\alpha\sigma e_0 s_0 + \alpha\sigma_{1_0} s_0 + \alpha\beta_1 i_0 s - \rho\sigma^2 e_0 \end{pmatrix}$$

This can be furthered till the desired number of iterations are obtained. Hence, the summary of iterative solutions to each model compartment is obtained as;

$S(t) = \sum_{k=0}^{3} s_k(t)\,, E(t) = \sum_{k=0}^{3} e_k(t)\,, I(t) = \sum_{k=0}^{3} i_k(t)\,, T(t) = \sum_{k=0}^{3} t_k(t)\,, R(t) = \sum_{k=0}^{3} r_k(t)\,, V(t) = \sum_{k=0}^{3} v_k(t),$

And evaluating these results using the corresponding model parameters of each class given by

$$\left.\begin{matrix} \alpha = 0.008, \delta = 0.4, \mu = 1.0, T = 0.1, \Lambda = 2.19, \gamma = 1.263, \beta = 0.002, \varepsilon = 0.03, \\ e_0 = 653930, s = 500000, i_0 = 23890, r_0 = 14730 \end{matrix}\right\} \quad (46)$$

It is therefore obtained that, the initial values of the model parameters results is defined by equation below;

$$\begin{aligned} S(t) &= 2700 - 103.84t + 0.82753t^2 - 0.00182736365t^3 \\ E(t) &= 81.2 + 773.12t - 127.27363t^2 + 0.8290276352t^3 \\ I(t) &= 16.7 - 0.0329t + 0.081522t^2 - 0.187263672365t^3 \\ T(t) &= 16.7 - 0.0329t + 0.081522t^2 - 0.187263672365t^3 \\ R(t) &= 11.2 - 0.02383t - 0.111827362t^2 + 1.282735836139t^3 \\ V(t) &= 142 - 0.8635t - 0.87379t^2 - 1.202372t^3 \end{aligned} \quad (47)$$

The approximate results of each class are evaluated using their respective baseline values in obtained from table 3. We also suggest the following population data set as initial values given by

$s_0 = 1327363, e_0 = 1923732, i_0 = 1112837, t_0 = 136833, r_0 = 2182733, v_0 = 717931$. Thus we obtain the following series of results embedding the parameters whose influence on the dynamics of measles transmission are to be analysed as;

$$S(t) = 1000 + \begin{pmatrix} 123.8273 + 1.9273\varepsilon \\ -1.8363\varepsilon^2 - 27.1\gamma \end{pmatrix} t + \begin{pmatrix} -71625.T^2 \\ +29.8635\mu^4 \\ 9272.86837 \\ +8126.916\alpha^2\gamma \end{pmatrix}\frac{t^2}{3} - \begin{pmatrix} 0.6621^2 c^2 - 1.82732\alpha^3 \\ -0.827252\delta^2 + 1.28263\alpha^4 \\ +18273.9273\alpha^2 + 817.282535 \\ -625422.753\alpha - 1.29233209 \\ +5243.91\mu^6 - 11.82636\gamma \end{pmatrix}\frac{t^3}{5}$$

$$E(t) = 30 + \begin{pmatrix} -23.3723648t \\ +0.003823646\alpha^2 \\ -12.8724643\alpha \end{pmatrix} t - \begin{pmatrix} -69.3086134\gamma \\ -0.181786136\varepsilon \\ +0.0938287\alpha^2 \\ +0.0000493608c \\ -5.292993669\alpha \end{pmatrix}\frac{t^2}{2} + \begin{pmatrix} 11.30828286\alpha^2 - 80.26339203\alpha^3 \\ -9.8173\alpha + 0.31334\alpha^4 c \\ -1.891383\alpha^3 c + 182.926\alpha^2 \\ +0.0.1753c - 16.8625\alpha \\ +1.23232\alpha^6 - 0.9021\alpha^5 \end{pmatrix}\frac{t^3}{7}$$

$$I(t) = 28 - 0.22133t - \begin{pmatrix} 127.0391180 \\ +0.63524\varepsilon^2 \\ -0.7283\gamma \end{pmatrix}\frac{t^2}{2} - \begin{pmatrix} -0.004499284709\varepsilon^3 + 320.2194878 \\ -0.138363\alpha + 4.407401276T^2 \\ +2.46825 \cdot 10^{-8}\beta - 0.004339725\beta \end{pmatrix}\frac{t^3}{3}$$

$$T(t) = 2763 - 0.98327t - \begin{pmatrix} 1379.81616 \\ +0.2634\varphi^2 \\ -0.7283\gamma_2 \end{pmatrix}\frac{t^2}{3} - \begin{pmatrix} -0.0089379\varepsilon^3 + 320.2194878 \\ -0.138363\alpha + 4.82726T^2 \\ +2..27623 \cdot 10^{-8}\beta - 0.092626\beta \end{pmatrix}\frac{t^3}{3}$$

$$R(t) = 40 + (46.18360 + 37.68c)t - \begin{pmatrix} 1817.52313 \\ +45.9850488T \\ -2044.386000\beta^2 \end{pmatrix}\frac{t^2}{3} + \begin{pmatrix} 13.49785413\alpha^3 - 8249.759899\alpha^4 \\ +262457 + 0.7236752367325\mu \\ +9.76026132237\beta^3 \end{pmatrix}\frac{t^3}{6}$$

$$V(t) = 28 - 0.22133t - \begin{pmatrix} 127.0391180 \\ +0.63524\varepsilon^2 \\ -0.7283\gamma \end{pmatrix}\frac{t^2}{2} - \begin{pmatrix} -0.004499284709\varepsilon^3 + 320.2194878 \\ -0.138363\alpha + 4.407401276T^2 \\ +2.46825 \cdot 10^{-8}\beta - 0.004339725\beta \end{pmatrix}\frac{t^3}{3}$$

RESULTS AND DISCUSSION

The interpretation of numerical simulation conducted through iterative steps using homotopy perturbation method is depicted pictorially below.

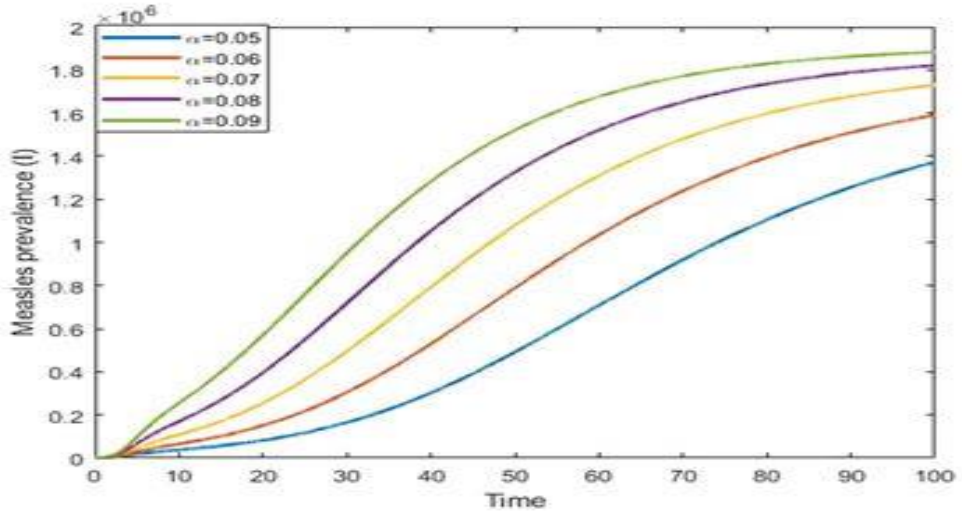

Figure 1: Impact of Vaccination Rate (α) on Measles Prevalence

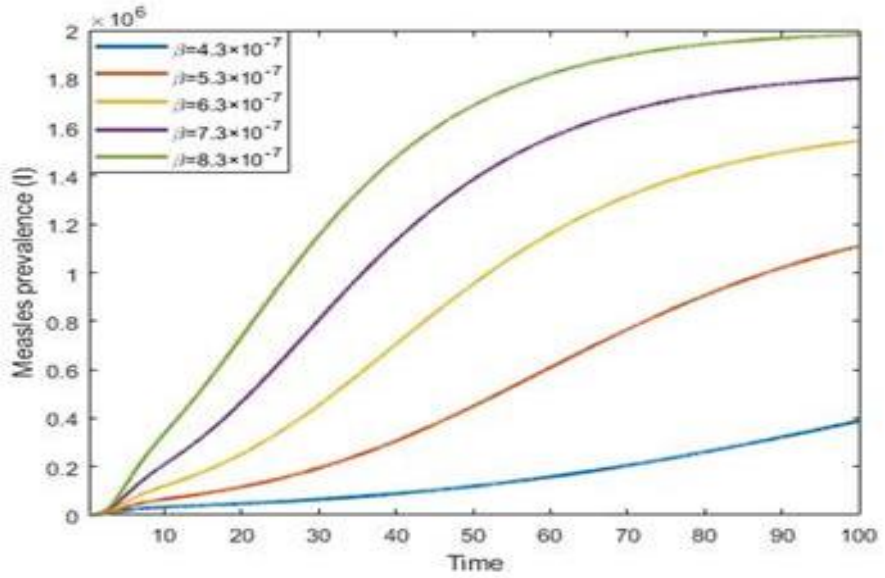

Figure 2: Impact of Progression Rate (ρ) on Measles Prevalence

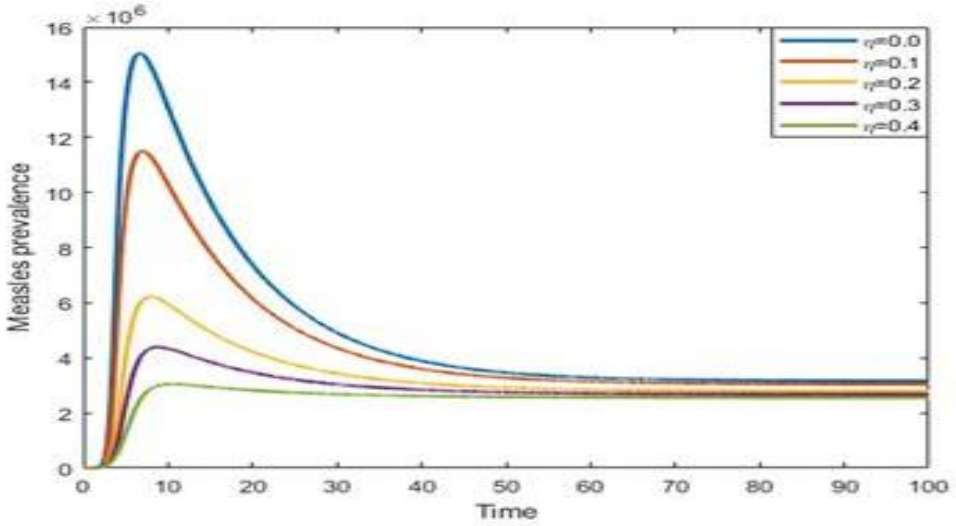

Figure 3: Impact of Treatment Rate (δ) on Measles Prevalence

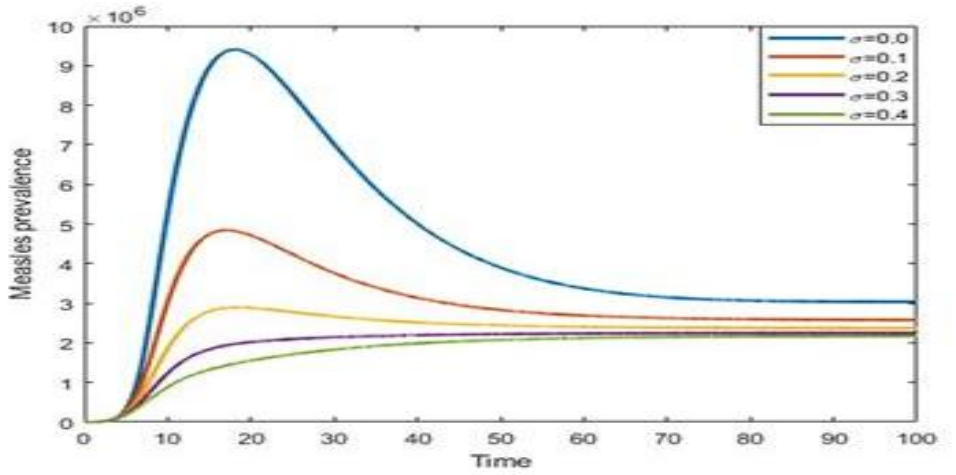

Figure 4: Impact of Treatment Rate (θ) on Measles Prevalence

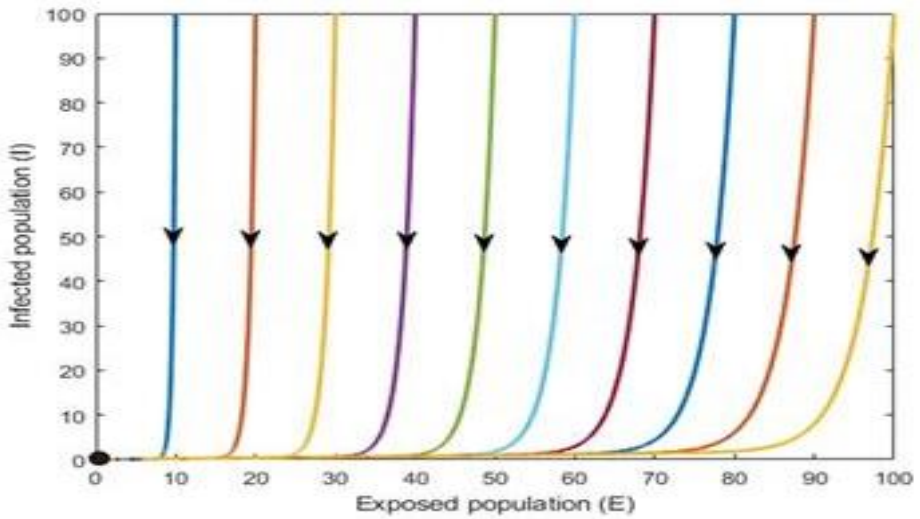

Figure 5: Infection at Equilibrium:$R_0 < 1$. In this case Measles Disease Dies out (Dark spot) with an Assumed Parameter Base Line

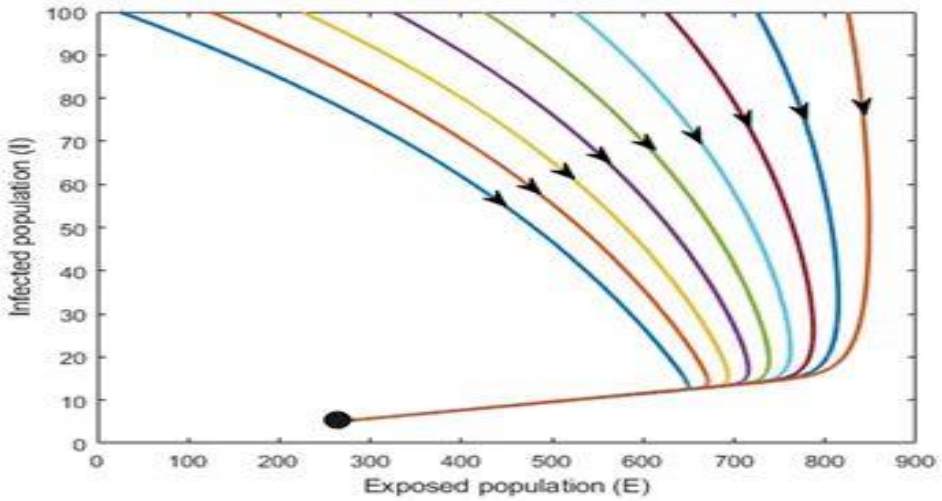

Figure 6: Endemic Equilibrium$R_0 > 1$. In this case Measles Disease Persist in the Population (dark spot) where all Parameter Values are Assumed for its Base Line

Discussion

The study points out that vaccination is essential for getting rid of measles. Although reaching high vaccination coverage is still vital, our findings suggest that other things like vaccine hesitancy increasing awareness and education play a major role in curbing disease spread. A combination of medical and behavioral measures is more successful in decreasing the number of measles infection cases and the death rate. These programs must be applied early and adequately for disease control to continue. For this research, Maple software was used to perform numerical simulations and visualize the effects of changing intervention parameters on the disease. The outcomes are shown in graphs and are thoroughly reviewed. Figure 1 shows that increasing vaccination rates lowers both the numbers of people who are not vaccinated and those who get the disease again, also the higher the vaccination rates, the fewer infected persons there are. Figure 2 proves that the number of infected cases lowers due to vaccination. From Figures 3 and 4 we deduce that increasing the number of people treated greatly reduces infections and when people receive enough vaccinations, the numbers of both infected and immunized individuals fall significantly, proving a strong link between treatment and vaccination.Figure5, 6 clearly show that in contrast, an endemic equilibrium means the disease continues in the system, mainly because the rate of vaccination used and the level of behaviors help to control how the disease spreads. Still, further highlighting the role of individual's plays helps reduce the numbers of people suffering from measles.

CONCLUSION

The method used in this paper is homotopy perturbation which led to the creation of a valid numerical answer describing the effects of strong treatment vaccination efficacy on measles. The model was able to give accurate predictions that led to the R0 of measles being found below unity for this approach. Numerical output was then run to see the effects of vaccination on measles within the population and detailed analysis of the graphs was done to understand the specific signals of both experimental and biological changes affecting different groups with time. Even so, using oral vaccine effectively and improving environmental cleanliness is useful for addressing the ongoing problem of measles and setting up strategies to prevent its spread and demolish in the short run. Raising awareness and providing information through education programs is very important for combating the spread of measles in the short run.

REFERENCES

Adewale, S. O., Mohammed, I. T., & Olopade, I. A. (2014). Mathematical analysis of effect of area on the dynamical spread of measles.

Adewole (2022). Modulating the Immune Response to Oncolytic Measles Viruses. Molecular Therapy, 9, S108. https://doi.org/10.1016/j.ymthe.2004.06.220

Kolawole, M. (2024). On the Numerical Simulation of the Effect of Disease Transmission Coefficient on SEIR Epidemic Model Using Hybrid Block Method. Jurnal diferensial, 6(1), 65-77.

Kolawole, M. K. (2025). Mathematical Dynamics of the (SVEITR) Model, the Impact of Treatment and Vaccination on Cholera Spread. Jurnal Diferensial, 7(1), 85-105.

Kolawole, M. K., & Olayiwola, M. O. (2016). On the Numerical Effect of Saturation Terms on the Susceptible Individual in Susceptible-Exposed-Infected-Recovered-Susceptible (SEIRS) Epidemic Model, computing information system Development informatics & Allied Research Journal, 7. Computing, information Systems, Development Informatics & Allied journal, 7(2), 83-90.

Kolawole, M. K., Alaje, A. I., Ogunniran, M. O., & Tijani, K. R. (2022a). Simulating the Effect of Disease Transmission Coefficient on A Disease Induced Death Seirs Epidemic Model Using the Homotopy Perturbation Method. Journal of Applied Computer Science & Mathematics, 16(33).

Kolawole, M. K., Odeyemi, K. A., Alaje, A. I., Oladapo, A. O., & Bashiru, K. A. (2022b). Dynamical analysis and control strategies for capturing the spread of covid-19. Tanzania Journal of Science, 48(3), 680-690.

Kolawole, M. K., Olayiwola, M. O., Alaje, A. I., Adekunle, H. O., & Odeyemi, K. A. (2023). Conceptual analysis of the combined effects of vaccination, therapeutic actions, and human subjection to physical constraint in reducing the prevalence of COVID-19 using the homotopy perturbation

method. Beni-Suef University Journal of Basic and Applied Sciences, 12(1), 10.

Kumar, M. L., Johnson, C. E., Chui, L. W., Whitwell, J. K., Staehle, B., & Nalin, D. (2022, Immune response to measles vaccine in 6-month-old infants of measles seronegative mothers. Vaccine, 16(20), 2047–2051. https://doi.org/10.1016/s0264-410x(98)00083-8

Oh, C., Rafai, E., Cho, Y., Jun, D., & Cha, S. (2022). An Economic Analysis of Mumps Vaccination in Fiji: Static Model Simulation of Routine Measles–Mumps–Rubella (MMR) Vaccination Instead of Current Measles–Rubella (MR) Vaccination. International Journal of Environmental Research and Public Health, 19(3), 2020. https://doi.org/10.3390/ijerph19031861

Olayiwola, M. O., Alaje, A. I., Yunus. A O, & Adedokun, K. A. (2023). A caputo fractional order epidemic model for evaluating the effectiveness of high-risk quarantine and vaccination strategies on the spread of COVID-19. Healthcare Analytics, 3, 100179

Olayiwola, M. O., Yunus, A. O., Ismaila, A., & Adedeji, J. A. (2025). Modeling within-host Chikungunya virus dynamics with the immune system using semi-analytical approaches. BMC Research Notes, 18(1), 1-15

Peter, O. J., Cattani, C., & Omame, A. (2024). Modelling transmission dynamics of measles: the effect of treatment failure in complicated cases. Modeling Earth Systems and Environment, 10(5), 5871-5889.

Phillipp, J. (2020). Alterations in immune response in acute measles and chronic post-measles in chest disease Coovadia, M., Wesley, A., Henderson, G., Brain, P., Vos, G., and Hallet, F.: Int. Arch. Allergy Appl. Immunol. 56:14, 1978. Journal of Allergy and Clinical Immunology, 62(4), B18. https://doi.org/10.1016/0091-6749(78)90223-3

Plans-Rubió, P. (2020). Are the Objectives Proposed by the WHO for Routine Measles Vaccination Coverage and Population Measles Immunity Sufficient to Achieve Measles Elimination from Europe? Vaccines, 8(2), 218. https://doi.org/10.3390/vaccines8020218

Suwoyo, S., Yani, E. R., & Hardjito, K. (2023). COVID-19 immune response in adults post Measles-Rubella vaccination. Vacunas, 24(4), 341–347. https://doi.org/10.1016/j.vacun.2023.05.004

Vynnycky, E., Papadopoulos, T., & Angelis, K. (2018). The impact of Measles-Rubella vaccination on the morbidity and mortality from Congenital Rubella Syndrome in 92 countries. Human Vaccines & Immunotherapeutics, 15(2), 309–316. https://doi.org/10.1080/21645515.2018.1532257

Wireko, F. A., Asamoah, J. K. K., Adu, I. K., & Ndogum, S. (2024). Non-optimal and optimal fractional control analysis of measles using real data. Informatics in Medicine Unlocked, 49, 101548.

Yunus, A. O., & Olayiwola, M. O. (2024). The analysis of a novel COVID-19 model with the fractional-order incorporating the impact of the vaccination campaign in Nigeria via the Laplace-Adomian Decomposition Method. Journal of the Nigerian Society of Physical Sciences, 1830-1830.

Yunus, A. O., & Olayiwola, M. O. (2025a). A mathematical model for assessing vaccination's efficacy as a preventative strategy against newly emerging COVID-19 variants. Vacunas, 500392

Yunus, A. O., & Olayiwola, M. O. (2025b). Epidemiological analysis of Lassa fever control using novel mathematical modeling and a dual-dosage vaccination approach. BMC Research Notes, 18(1),

Yunus, A. O., & Olayiwola, M. O. (2025c). Simulation of a novel approach in measles disease dynamics models to predict the impact of vaccinations on eradication and control. Vacunas, 100385.

Yunus, A. O., & Olayiwola, M. O.(2025d). Dynamics of Ebola virus transmission with vaccination control using Caputo-Fabrizio Fractional-order derivative analysis. Modeling Earth Systems and Environment, 11(3),